

RESEARCH ARTICLE | JANUARY 18 2024

On estimating key cloud properties with satellite observations: An artificial intelligence based retrieval framework **FREE**

Pietro Mastro ✉; Domenico Cimini; Filomena Romano; Elisabetta Ricciardelli; Francesco Di Paola; Salvatore Larosa; Tim Hultberg; Thomas August; Carmine Serio; Guido Masiello



AIP Conf. Proc. 2988, 040002 (2024)

<https://doi.org/10.1063/5.0187904>



Boost Your Optics and Photonics Measurements

Lock-in Amplifier

Zurich Instruments

Find out more

Boxcar Averager

On Estimating Key Cloud Properties With Satellite Observations: An Artificial Intelligence Based Retrieval framework

Pietro Mastro^{1, a)} Domenico Cimini, Filomena Romano², Elisabetta Ricciardelli², Francesco Di Paola², Salvatore Larosa², Tim Hultberg³, Thomas August³, Carmine Serio¹, Guido Masiello¹.

¹University of Basilicata, School of Engineering, Via Ateneo Lucano 2, 85100, Potenza, Italy;

²National Research Council of Italy, Institute of Methodologies for Environmental Analysis (CNR-IMAA), Contrada Loya, 85050, Tito, Italy;

³European Organisation for the Exploitation of Meteorological Satellites (EUMETSAT), Allee 1, 64295, Darmstadt, Germany.

Author Emails

^{a)} Corresponding author: pietro.mastro@unibas.it

Abstract. This work builds on the analyses made within the EUMETSAT ComboCloud project (contract EUM/CO/19/4600002352/THH) whose purpose was to develop AI-based solutions to infer key cloud parameters exploiting the combination of innovative features offered by upcoming satellite sensors, namely the Next Generation Atmospheric Sounding Interferometer (IASI-NG), and the Microwave Sounder (MWS). We present the potential of the developed solutions applied to real observations, from the instruments flying onboard the EUMETSAT MetOp satellites such as the Atmospheric Sounding Interferometer (IASI), the Advanced Microwave Sounding Unit (AMSU), and the Microwave Humidity Sounder (MHS) and validated against cloud products from an independent dataset of real observations. The validation demonstrated good agreement between reference and retrieved cloud key parameters, showing consistent range and spatial patterns.

INTRODUCTION

Over the last three decades using instruments operating in visible, infrared, and microwave bands, a variety of tools have been developed to retrieve cloud microphysics properties¹⁻³. In this work, we show the potential of an AI-based regression framework for the estimation of cloud microphysical parameters by the synergic use of observation in the microwave and the infrared bands. Here, the addressed key cloud parameters are the vertical profiles of cloud liquid water content (CLWC) and cloud ice water content (CIWC), their column-integrated values, cloud liquid water path (CLWP) and cloud ice water path (CIWP), and finally the cloud drop effective radius (r_e). The next sections will introduce the database of measurements used in this work. In the following, the architecture of the developed framework will be briefly discussed. Finally, the evaluation of the regression performance obtained in validation will be shown.

INFRARED AND MICROWAVE DATA

A simulated dataset of realistic sea surface observations was produced by processing global data from ERA5, which is the fifth generation of the European Center of Medium-range Weather Forecast (ECMWF) reanalysis, with state-of-the-art radiative transfer models (RTM) codes. Namely, RTTOV-SCATT⁴ and σ -IASI-as^{5,6} (with new cloud parametrization⁷) codes were exploited for the simulation of microwave (MW) and infrared (IR) satellite observations.

Specifically, sensors of the Meteorological Operational Satellites of the first generation (MetOp-FG) including i) the Infrared Atmospheric Sounding Interferometer (IASI), ii) the Advanced Microwave Sounding Unit A (AMSU-A), and iii) the Microwave Humidity Sounder (MHS) are the sensors involved.

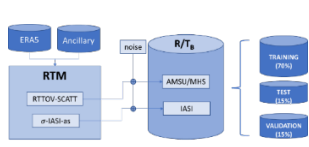


FIGURE 1. Processing scheme of the simulated dataset of IR (IASI) and MW (AMSU and MHS) measurements.

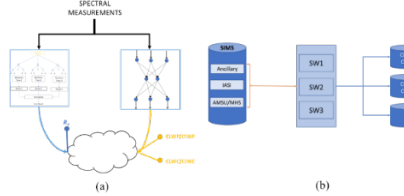


FIGURE 2. (a) Simple sketch of the AI inversion approach used for the regression of cloud microphysical parameters. (b) Regression framework implemented architecture.



FIGURE 3. Regression architectures of (a) SW1, (b) SW2 and (c)-(d) SW3 processors.

The radiation measured by these sensors interacts with cloud particles in such a way that the greatest sensitivity to its microphysical details occurs when the wavelength of the radiation is close to the size of the particles and in this way more or less sensitive to the amount of ice and liquid water particles in the clouds and their burden. A synergy of observed IR and MW measurements needs to be investigated. Global data have been simulated accordingly to what is presented in ⁸⁻¹⁰. Figure 1 shows a summary of the process for the generation of the dataset of satellite measurements.

METHOD AND REGRESSION FRAMEWORK ARCHITECTURE

In this work, AI is the core of the inversion framework developed. Specifically, we adopted two types of AI inversion approaches, namely the feed-forward Neural Networks (NN)^{11,12} and the random forests (RF)¹³ (see Figure 2 (a)). The NN inversion approach was adopted for the retrieval of CLWC, CIWC profiles, and their vertical integrated paths (CLWP and CIWP). RF algorithm was adopted for the retrieval of drop effective radius of liquid water and ice clouds. Thus, three independent processors namely SW1, SW2, and SW3 have been implemented (see Figure 2 (b)). Details about data processing and SW regression schemes (see Figure 3) can be found in Mastro et al. ⁸⁻¹⁰. Finally, in the next sections, the evaluation of the regression performance obtained in validation by the implemented SW processors is presented using simulated and real observations (e.g., MetOp-FG real observation collocated with the ECMWF analysis dataset).

VALIDATION WITH A DATASET OF SIMULATIONS

The remaining 15% of the total dataset of simulated measurements has been used for the validation step of the developed SWs. For the SW1 processor, here we show some results related to coordinates in the tropics area.

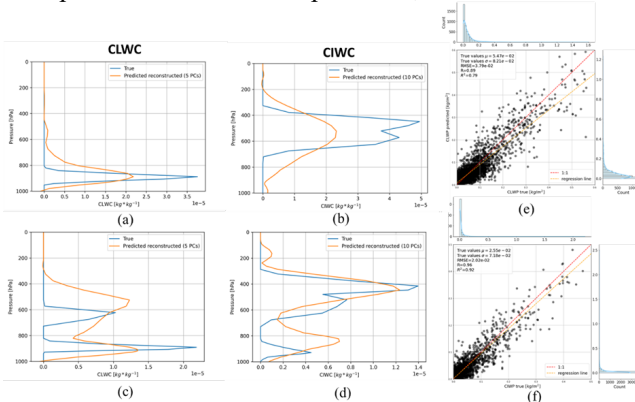


FIGURE 4. (a)-(d) Reference vs predicted CLWC and CIWC profiles. (e) CLWP scatter plot between reference and predicted CLWC. (f) CIWP scatter plot between reference and predicted CIWC.

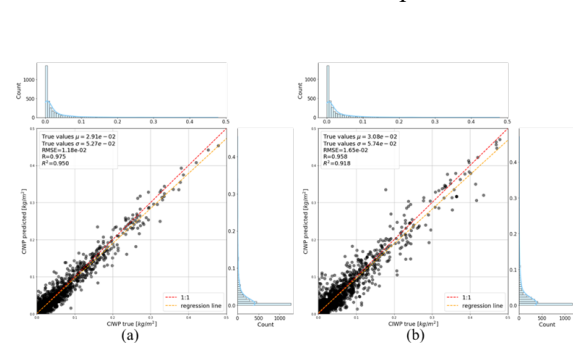


FIGURE 5. Scatter plots of (a) CLWP and (b) CIWP.

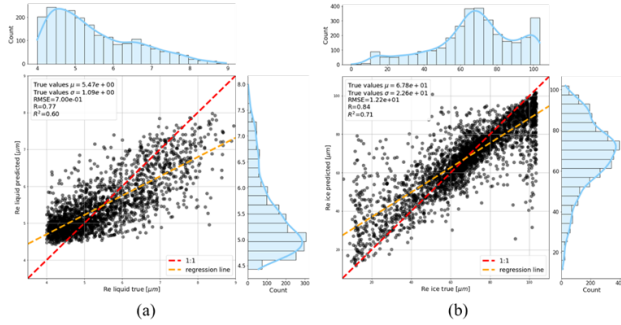


FIGURE 6. Scatter plots of (a) liquid water and (b) ice clouds effective radii.

TABLE 1. Retrieval performance evaluation of SW processors with respect to the WMO OSCAR database

PRODUCT	UNITS	Thresh.	Breakthr.	Objective	ComboCloud	
CLWP from (CLWC)	g/m ²	50 g/m ²	20 g/m ²	10 g/m ²	38 g/m ²	SW1
CIWP from (CIWC)	g/m ²	20 g/m ²	10 g/m ²	5 g/m ²	20 g/m ²	
CLWP	g/m ²	50 g/m ²	20 g/m ²	10 g/m ²	22 g/m ²	SW2
CIWP	g/m ²	20 g/m ²	10 g/m ²	5 g/m ²	17 g/m ²	
Re	μm	5 μm	2 μm	1 μm	0.7 μm (liq) 12.2 μm (ice)	SW3

The results shown in Figures 4 (a)-(d) demonstrate that the prediction of the PCs of CLWC and CIWC from the SW1 processor allows a reasonable reconstruction of the corresponding profiles. The goodness of SW1 predictions is also demonstrated by analyzing R^2 values from the CLWP and CIWP scatter plots (see Figure 4 (e)-(f)). Concerning the SW2 processor, also the R^2 scores are high (see Figures 5 (a) and (b)) demonstrating very good retrieval performances. Finally, in Figure 6 we show the scatter plots of SW3 regressions of ice and liquid water cloud drop effective radii. Moderate values of R^2 are obtained, highlighted by comparing the marginal histograms between reference and predicted values which have very similar skewness and median values. Finally, in Table 1 SWs regression performance was evaluated using the Numerical Weather Prediction (NWP) requirements of the World Meteorological Organization (WMO) OSCAR database. The performances for the integrated liquid and ice paths both for SW1 and SW2 are between the threshold and breakthrough levels, more in agreement for SW2. For the retrieval of effective radius Re , the achieved performances meet the objective level when limited to liquid clouds. For ice clouds, currently, no information is available within the WMO OSCAR database to track the requirements of the drop effective radius of ice clouds. Therefore, such measurements may be considered a new result.

VALIDATION ON A DATASET OF REAL OBSERVATION

Here we present the validation of our models on real observations. To have a cross-validation dataset covering the whole range of latitude we collocated measurements from MetOp-B and MetOp-C platforms with ECMWF analyses measurements (MARS system) from 8 September 2021 to 10 September 2021. Among these, we selected the measurements within +/- 30 minutes from the ECMWF analysis base time. A subset of about four hundred thousand sea surface acquisitions was used for the validation. We made a spatial comparison between SW predictions and reference ECMWF values. Specifically, we selected a specific area from low- to mid-latitudes.

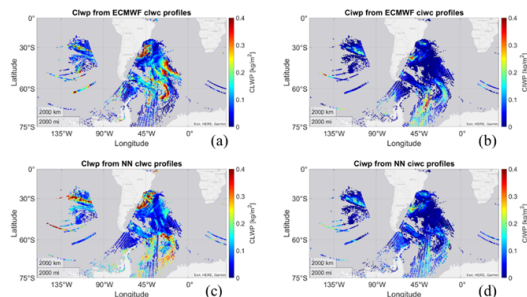


FIGURE 7. Spatial comparison between ECMWF and SW1 CLWP (a)-(c) and CIWP (b)-(d) values.

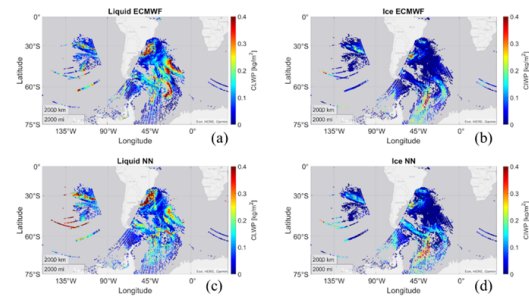


FIGURE 8. Spatial comparison between ECMWF and SW2 CLWP (a)-(c) and CIWP (b)-(d) values.

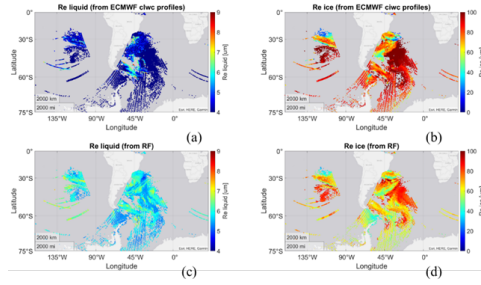


FIGURE 9. Spatial comparison between ECMWF and SW3 liquid water (a)-(c) and ice (b)-(d) cloud drop effective radii values.

Figure 7 shows the comparison between SW1 and ECMWF in terms of CLWP (a)-(b) and CIWP (c)-(d) values where good spatial agreement is revealed. Into the same area (see Figure 8), the goodness of the SW2 processor can also be appreciated. In this case, the CLWP and CIWP predictions follow the reference ECMWF spatial dynamics closely, better than the SW1 processor, as expected. Finally, also for the SW3 processor, a fair agreement of the spatial pattern is observed. See Figure 9.

CONCLUSION

In this work, we presented the potential of an AI-based inversion framework for the regression of key cloud parameters by the synergic use of MW and IR measurements. Validation performance on simulated measurement results in agreement with the WMO OSCAR requirements for global NWP applications. Validation with real observations shows consistent results in terms of spatial dynamics.

ACKNOWLEDGMENTS

IASI has been developed and built under the responsibility of the Centre National d'Etudes Spatiales (CNES, France). IASI, AMSU-A, and MHS instrumentations fly onboard the Metop satellites as part of the EUMETSAT Polar System. This work is supported by EUMETSAT under contract EUM/CO/19/460002352/THH.

REFERENCES

1. M. Dowell, P. Lecomte, R. Husband, J. Schulz, T. Mohr, Y. Tahara, R. Eckman, E. Lindstrom, C. Wooldridge, S. Hilding, J. Bates, B. Ryan, J. LaFeuille, and S. Bojinski, *Strategy Towards an Architecture for Climate Monitoring from Space* (2013).
2. B. Lin, P. Minnis, B. Wielicki, D.R. Doelling, R. Palikonda, D.F. Young, and T. Uttal, *Journal of Geophysical Research: Atmospheres* **103**, 3887 (1998).
3. T.T. Wilheit and K.D. Hutchison, *IEEE Transactions on Geoscience and Remote Sensing* **38**, 1253 (2000).
4. R. Saunders, J. Hocking, E. Turner, P. Rayer, D. Rundle, P. Brunel, J. Vidot, P. Roquet, M. Matricardi, A. Geer, N. Bormann, and C. Lupu, *Geosci. Model Dev.* **11**, 2717 (2018).
5. G. Liuzzi, M.G. Blasi, G. Masiello, C. Serio, and S. Venafra, in (Auckland, New Zealand, 2017), p. 040004.
6. U. Amato, G. Masiello, C. Serio, and M. Viggiano, *Environmental Modelling & Software* **17**, 651 (2002).
7. M. Martinazzo, D. Magurno, W. Cossich, C. Serio, G. Masiello, and T. Maestri, *Journal of Quantitative Spectroscopy and Radiative Transfer* **271**, 107739 (2021).
8. P. Mastro, G. Masiello, D. Cimini, F. Romano, E. Ricciardelli, F.D. Paola, T. Hultberg, and T. August, in *Remote Sensing of Clouds and the Atmosphere XXVI* (SPIE, 2021), pp. 52–64.
9. P. Mastro, G. Masiello, C. Serio, D. Cimini, E. Ricciardelli, F.D. Paola, T. Hultberg, T. August, and F. Romano, *IEEE Journal of Selected Topics in Applied Earth Observations and Remote Sensing* **15**, 3313 (2022).
10. P. Mastro, D. Cimini, F. Romano, E. Ricciardelli, F. Di Paola, G. Masiello, and C. Serio, in *Remote Sensing of Clouds and the Atmosphere XXVII*, edited by A. Comerón, E.I. Kassianov, K. Schäfer, R.H. Picard, K. Weber, and U.N. Singh (SPIE, Berlin, Germany, 2022), p. 29.
11. I. Goodfellow, Y. Bengio, and A. Courville, *Deep Learning* (The MIT Press, Cambridge, Massachusetts, 2016).
12. K. Hornik, M. Stinchcombe, and H. White, *Neural Networks* **2**, 359 (1989).
13. L. Breiman, *Machine Learning* **45**, 5 (2001).